THE ASTROPHYSICAL JOURNAL, 412:797–809, 1993 August 1

THE FUNDAMENTAL PARAMETERS OF THE CHROMOSPHERICALLY ACTIVE K2 DWARF ϵ ERIDANI

JEREMY J. DRAKE[1,2,3] AND GEOFFREY SMITH[1]

Received 1992 July 1; accepted 1993 February 9

ABSTRACT

Regions exhibiting calcium and iron lines in the spectrum of the chromospherically active K2 dwarf ϵ Eri have been recorded at a resolution of $\lambda/\Delta\lambda = 120{,}000$ and with signal-to-noise ratio ≥ 200 using a silicon array detector. A fine analysis of the resulting spectra has yielded the following fundamental parameters:

Effective temperature: $T_{\rm eff} = 5180 \pm 50$ K

Surface gravity: $\log g = 4.75 \pm 0.1$ dex

Logarithmic iron abundance (relative to the Sun): [Fe/H] $= -0.09 \pm 0.05$

Logarithmic calcium abundance (relative to H = 12.00): Ca/H $= 6.26 \pm 0.05$

Microturbulence: $\xi = 1.25 \pm 0.1$ km s^{-1}.

Three high-excitation lines of Fe I were found to yield anomalously low iron abundances; it is postulated that the origin of the anomaly lies in nonthermal excitation of the upper photosphere caused by chromospheric emission.

A comparison between the observed profile of the very strong Ca II 8542 Å line and theoretical profiles calculated using different model atmospheres has confirmed that a scaled solar model, based on the Holweger & Müller solar model, provides an optimal $T(\tau)$ relation for ϵ Eri.

Our fundamental parameters have been used to demonstrate that ϵ Eri is in an evolutionary stage consistent with an $M/M_{\odot} = 0.85$ theoretical zero-age main-sequence model. Considered with the existing evidence of high chromospheric activity and brisk rotation, our results suggest that ϵ Eri is almost certainly a young star of slightly less than one solar mass.

Subject headings: stars: atmospheres — stars: chromospheres — stars: individual (ϵ Eridani) — stars: late-type

1. INTRODUCTION

The nearby K2 dwarf ϵ Eri ($V = 3.73$) has been the subject of numerous observational campaigns in recent years. Many of these have involved studies of chromospheric activity: see Thatcher, Robinson, & Rees (1991), Jordan et al. (1987), Simon, Kelch, & Linsky (1980), Kelch (1978), and references cited therein. Other workers have attempted to study the surface magnetic field either through broad-band polarimetry (Leroy & Le Borgne 1989) or through Zeeman broadening of spectral line shapes (Mathys & Solanki 1989; Marcy & Basri 1989; Marcy 1984; see Saar 1988 for a representative discussion of the method employed). Among more exotic investigations, ϵ Eri features in the search of Campbell, Walker, & Yang (1988) for substellar companions to solar-type stars and has also attracted attention as a possible candidate for stellar oscillation studies. Noyes et al. (1984) claimed to have discovered a periodic modulation of the Ca II H and K emission, an observation which has subsequently been discussed in terms of global p-mode oscillations (Soderblom & Däppen 1989; Guenther 1987; Guenther & Demarque 1986). ϵ Eri is also one of the nearby stars found to have a far-infrared excess from *IRAS* observations, suggesting the presence of dusty material of approximately solar system dimensions (Gillet 1986; Walker & Wolstencroft 1988).

Despite all of the intriguing astrophysical problems posed by ϵ Eri, there have been very few convincing measurements of this star's stellar parameters $T_{\rm eff}$, $\log g$, and metallicity (usually represented by [Fe/H], the logarithmic abundance of iron relative to that of the Sun). Cayrel de Strobel et al. (1985) list three previous spectroscopic abundance analyses, namely those of Hearnshaw (1974), Oinas (1974a, b), and Steenbock (1983). Since 1985 only Abia et al. (1988) have attempted to derive [Fe/H] spectroscopically, using seven Fe I lines. Other studies have determined one or more of the parameters by various means; we list them here in brief. Krishna Swamy (1966) used the wings of the Hα, Ca II H, K and infrared triplet, and Na D lines to constrain the metallicity and effective temperature simultaneously, and used this temperature to derive a surface gravity from a $M_{\rm bol}$ and a mass-luminosity relation. Kelch (1978) derived an effective temperature from broad-band colors and estimated a surface gravity using theoretical evolutionary tracks. Tomkin & Lambert (1980) determined a photometric temperature and arbitrarily chose a value for the surface gravity. Burnashev (1983) determined an effective temperature, surface gravity and iron abundance from observations of the spectral energy distribution of ϵ Eri. Abia et al. (1988) derived an effective temperature and surface gravity using narrow-band color indices. Arribas & Martinez Roger (1989) arrived at an effective temperature via their color calibration and existing photometry. Finally, Bell & Gustafsson (1989) derived a temperature using a version of the infrared flux method (hereafter

[1] Department of Physics, Nuclear and Astrophysics Laboratory, University of Oxford, Keble Road, Oxford OX1 3RH, UK.

[2] Also Astronomy Department, University of Texas at Austin.

[3] Postal address: Center for EUV Astrophysics, University of California, 2150 Kittredge Street, Berkeley, CA 94720.

TABLE 1

A SUMMARY OF SOME DETERMINATIONS OF THE PARAMETERS OF ϵ ERIDANI[a]

$T_{\rm eff}$ (K)	log g	[M/H]	ξ	Reference
5050^{w}	4.565^{e}	0.0^{w}	...	Krishna Swamy 1966
5020^{p}	4.61^{e}	−0.31^{s}	1.3	Hearnshaw 1974
5000^{p}	(4.4^{a}, 3.6^{i})[b]	−0.19^{s}	2.3	Oinas 1974a, b
5000^{p}	4.5^{e}	...	...	Kelch 1978
5100^{p}	4.5^{a}	...	...	Tomkin & Lambert 1980
5040^{p}	4.1^{i}	−0.20	1.9	Steenbock & Holweger 1981
5000^{f}	4.8^{f}	−0.08^{f}	...	Burnashev 1983
5040^{p}	4.19^{i}	−0.23^{s}	1.8	Steenbock 1983
4990^{p}	4.8^{p}	−0.2^{s}	...	Abia et al. 1988
4990^{p}	...	...	...	Arribas & Martinez Roger 1989
5156^{ri}	(4.61^{p})[c]	(0.05^{p})[c]	...	Bell & Gustafsson 1989
5180^{i}	4.75^{w}	−0.09^{s}	1.25	This work

[a] The superscipts denote the methods used (also refer to text): (*a*) arbitrarily adopted value; (*e*) estimated from theoretical evolutionary tracks; (*f*) derived from the flux distribution; (*i*) from the Fe I–Fe II ionization balance; (*p*) from photometric material; (*ri*) renormalized infrared flux method; (*s*) spectroscopic abundance; (*w*) determined from the wings of strong lines.

[b] Oinas determined log g = 3.6 spectroscopically, but adopted the higher value.

[c] Values from Frisk 1983.

IRFM) (Blackwell et al. 1986) and quote a gravity and metal abundance from the narrow-band work of Frisk (1983). This potpourri of results is summarized in Table 1.

A glance at this literature reveals a rather unsatisfactory situation. Although the effective temperature of ϵ Eri appears to be reasonably well determined by photometry, with relatively little scatter in the results listed in Table 1, many values were derived from the same photometric material, using similar color calibrations; the general agreement is not therefore surprising. Apart from the early line profile analysis of Krishna Swamy, the temperature has not been confirmed spectroscopically. The surface gravities cited exhibit a scatter of a factor of 5; the only noteworthy spectroscopic estimates to date, by Steenbock (1983), and Steenbock & Holweger (1981), are the lowest of these values. The spectroscopically determined metallicites appear to be in agreement. However, ϵ Eri's metallicity and age are still maters of controversy. The presence of circumstellar dust might or might not be indicative of youth: Aumann (1985) notes that among the nearby stars exhibiting a far-infrared excess there is preponderance of A and F stars, suggesting an effect common to relatively young stars, but warns that luminosity and brightness selection effects could also produce such a distribution. Guenther (1987) describes a dichotomy between the apparently subsolar metallicity, which suggests old age (see, for example, Twarog 1980), and the high chromospheric activity and "rapid" rotation (2–3 times solar), which are indicative of youth (Skumanich 1972; see, for example, Barry, Cromwell, & Hege 1987, and Bohigas et al. 1986, for more recent discussions). The stellar model adopted by Guenther & Demarque (1986), which fits the oscillation spectrum reported by Noyes et al. (1984) without resorting to arbitrary mixing-length parameters, implies an age of over 20 Gyr. Conversely, Soderblom & Däppen (1989) consider the high chromospheric activity as constraining the age to $\sim$1 Gyr; in order then to match the purported oscillation spectrum, their model required a very low value for the mixing length ($\alpha \approx 0.5$). This situation can be resolved only when more accurate values for the fundamental parameters have been determined. Soderblom & Däppen conclude that a "concerted effort must be made to improve our knowledge of the fundamental parameters of likely targets for efforts to detect stellar oscillations."

Since a prerequisite for any quantative interpretation of stellar spectral and oscillatory features is a knowledge of the stellar parameters effective temperature, surface gravity, and metallicity, additional effort to determine these parameters with high precision is very desirable. Smith & Drake (1987) have demonstrated that it is possible to determine self-consistently the parameters $T_{\rm eff}$, log g, iron abundance relative to the Sun [Fe/H], and calcium abundance Ca/H, with high precision in solar-type dwarfs using a limited set of high quality observations of Ca and Fe lines. In this paper, we report the results of a similar approach to ϵ Eri. Our analysis is based on Reticon spectra of very high quality and follows closely that described by Smith & Drake, with special attention paid to possible complications due to chromospheric activity. We also discuss briefly the evolutionary status of ϵ Eri in the light of our newly derived stellar parameters.

2. OBSERVATIONS

Observations of ϵ Eri were made in 1986 December at the McDonald Observatory, University of Texas, with the 2.7 m telescope and coudé spectrograph equipped with a 1872 diode Reticon detector (Vogt, Tull, & Kelton 1978). Five spectral regions covering approximately 25 Å each and centered on 5260, 5861, 6153, 6167 and 6447 Å were observed. A supplementary observation of an additional region, centered on 6501 Å, was kindly made for us in February of 1987 by V. V. Smith (University of Texas). These regions were chosen because they feature a number of calcium lines with relatively unblended profiles, for which there exists a fairly extensive set of accurate laboratory data (Smith 1988; Smith & Raggett 1981; and references therein). The same regions also exhibit a number of unblended iron lines suitable for analysis. The observations employed an echelle grating giving a dispersion varying between 0.012 Å per diode (15 μm) at 5260 Å in the 43d order, and 0.015 Å per diode at 6500 Å in the 35th order. The required order of the echelle spectrum was isolated by means of a grating monochromator directly in front of the spectrograph slit. This arrangment, in which only about 50 Å of spectrum

enters the main spectrograph, is particularly effective in reducing the scattered light background. The entrance slit width of 240 μm projected onto 3.6 diodes in the focal plane, giving a limit of resolution of $\simeq$0.05 Å. Integration times of approximately 150 minutes yielded excellent spectra with signal-to-noise ratio $\simeq$200 or greater. A typical example of the spectra obtained is illustrated in Figure 1.

In addition to the above, an observation of the strong, collisionally broadened Ca II 8542 Å line was made in 1987 January, by J. Tomkin (University of Texas). Since the broad wings of this line extend to at least 25 Å each side of the line center, a conventional grating was employed which gave a spectral range of approximately 100 Å on the Reticon, at a dispersion of 0.053 Å per diode in the first order. A color filter was used to eliminate second-order light. This arrangement provided sufficient resolution to allow reliable identification of blends, and sufficient spectral range to include all of the line wings, thereby permitting accurate continuum location. An integration time of 30 minutes gave a spectrum with signal-to-noise ratio $\simeq$300.

Diode-to-diode sensitivity variations were eliminated in all the stellar spectra by applying a flat-field correction. For this purpose, the spectrum of a tungsten filament lamp was recorded immediately after each stellar integration, at the same grating setting.

3. DATA REDUCTION

3.1. *Line Selection*

The calcium and iron lines selected for use in the analysis are listed in Table 2. Any lines thought to be significantly affected by blends were rejected. The methods of line selection and equivalent width measurement employed have been described in detail in previous papers (Drake & Smith 1991; Smith & Lambert 1983) and will only be related here in brief.

As a rough guide, the line selection procedure can be summarized by three criteria: (1) blends must not affect the line profile to a depth greater than 20% of the total line depth, as measured from the continuum; (2) lines appearing clean but with anomalously large widths or asymmetries are rejected; (3) the estimated total combined equivalent width of coincident lines listed by Kurucz & Peytremann (1975) most not exceed 1 mÅ. At the resolution of our echelle spectra, Gaussian profiles are a poor approximation to stellar line profiles exhibited by late-type dwarfs. Therefore, to aid (1) and (2), above, an analytical profile is calculated to fit each observed profile using an appropiate model atmosphere and realistic line-broadening parameters. When observed and analytical profiles are compared, asymmetries and hidden blends become readily apparent, and the severity of any blends in the observed line wings can be quantitatively estimated. In some cases when profiles are compared, one wing of the observed profile follows the analytical profile closely, while the other wing is too broad, indicating the presence of a weak blend. Provided (1), above, is satisfied, the line is retained and the weak blend in the wing is removed by assuming that the true line wings can be approximated by the analytical shape.

3.2. *Equivalent Widths*

In the case of ϵ Eri, the equivalent widths of the profiles, deblended as described above, were measured using the interactive C-program WIDTH, devised by A. Booth. These equivalent widths are also listed in Table 2, together with the oscillator strengths adopted for the various lines. Calcium *gf*-values were taken from Smith (1988) and Smith & Raggett (1981). Since accurate and reliable oscillator strengths are not yet available for Fe I lines of moderate and high excitation ($\chi > 2.6$ eV) and Fe II lines, "solar" oscillator strengths were derived for the complete set of iron lines from the digital version of the Kitt Peak solar flux atlas (Kurucz et al. 1984). Equivalent widths were measured in the manner described above, and oscillator strengths calculated using the Holweger & Müller (1974) solar model atmosphere. A solar iron abundance of Fe/H = 7.50 (on the logarithmic scale relative to H = 12.00) and a depth-independent microturbulence of 1.5 km s^{-1}, based on the analysis of solar Ca I lines of moderately high excitation (Smith, Edvardsson, & Frisk 1986), were assumed. The value of the solar iron abundance adopted is of

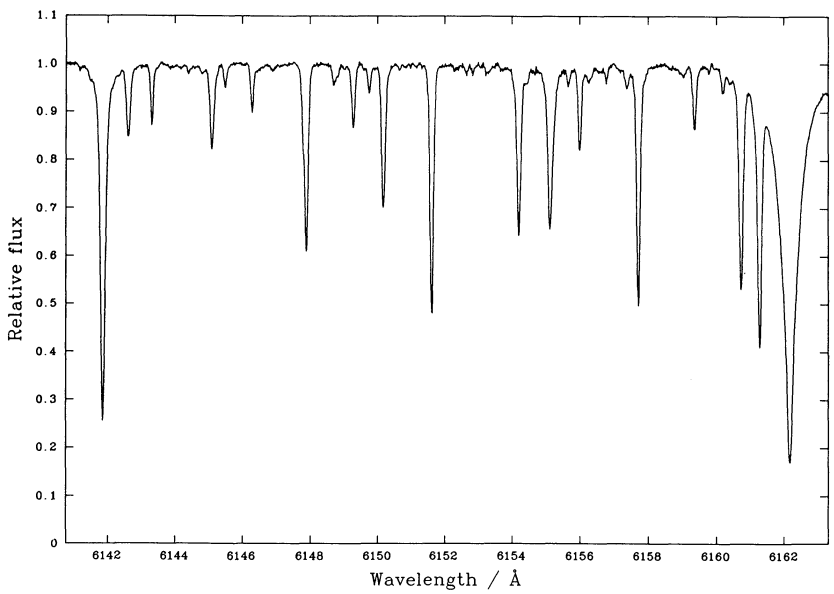

FIG. 1.—The 6150 Å region in ϵ Eri

TABLE 2

ATOMIC DATA AND EQUIVALENT WIDTHS FOR Fe AND Ca LINES

Species[a]	Wavelength (Å)	Excitation (eV)	log *gf* (D)[b]	log *gf* (S)[c]	Equivalent Width (D)[b]	Equivalent Width (S)[c]
Ca I	5260.39	2.52	−1.72		51	
	5867.57	2.93	−1.57		39	
	6161.29	2.52	−1.27		94	
	6166.44	2.52	−1.14		104	
	6169.04	2.52	−0.80		141	
	6455.60	2.52	−1.34		76	
	6493.78	2.52	−0.11		185	
Fe I	5253.03	2.28	−3.81		31	
	6151.62	2.18	−3.32		67	
	6173.34	2.22	−2.94		93	
	6498.95	0.96	−4.63		70	
	5852.23	4.55	−1.20	−1.16	48	50
	5855.09	4.61	−1.52	−1.53	28	24
	5856.10	4.29	−1.55	−1.50	39	45
	5858.79	4.22	−2.17		17	
	5859.60	4.55	−0.60	−0.64	82	90
	5862.37	4.55	−0.39	−0.40	103	112
	6157.73	4.08	−1.21		67	
	6159.38	4.61	−1.85		16	
	6165.36	4.14	−1.47		49	
Fe II.....	5264.81	3.23	−3.20	−3.24	24	33
	6149.25	3.89	−2.81		17	
	6456.39	3.90	−2.24		37	

[a] The log *gf* values for the set of Fe lines were derived from the solar spectrum (refer to text); the log *gf* values for the set of Ca lines are based on laboratory measurements (Smith 1988; Smith & Raggett 1981).

[b] Lines used in the analysis (D).

[c] Data from Steenbock 1983 (S).

no significance for present purposes, since the analysis demands only a knowledge of the photospheric iron abundance for ϵ Eri relative to that in the Sun.

Unfortunately, there are very few lines in our sample for which there exist equivalent widths published by earlier workers. Oinas (1974a, b) neglected to list the lines and equivalent widths used in his analysis. A handful of the lines used by Steenbock (1983) appear in our sample; his equivalent widths are also listed in Table 2, together with his "solar" log *gf*-values. To derive the latter, we have subtracted our adopted solar iron abundance, Fe/H = 7.50, from the log *gfa* (where *a* represents iron abundance) values listed by Steenbock. It is interesting to note that, with the exception of the 5855 Å Fe I and 5264 Å Fe II lines, Steenbock's equivalent widths are larger than our own by $\sim 10\%$. A similar discrepancy was noted by Drake & Smith (1991) in a comparison of their equivalent widths and those of Ruland et al. (1980), for the spectrum of the K0 giant Pollux. They attributed the discrepancy to a different treatment of blends in the line wings. Since even some of the cleanest lines in the spectrum of a K2 dwarf are inevitably contaminated to a small extent by weak blends in the region of the line wings, we feel confident that a similar situation exists here. This conclusion is strongly reinforced when we compare our equivalent widths measured from the less crowded solar spectrum with those of Steenbock: both sets are in excellent agreement, differing by less than 5%. Consequently, it is encouraging that the two sets of "solar" log *gf*-values listed in Table 2 are also in excellent agreement, differing by ≤ 0.04 dex. This result indicates that no significant differences exist between results derived from the different computer codes used in the two analyses. Equivalent widths for our set of lines in ϵ Eri have also been measured independently, using different software, by another worker. These measurements vindicate our own, differing by less than 5% (M. J. Ruck, private communication).

4. ANALYSIS

The stellar parameters were determined in a self-consistent way using the equivalent widths of a limited set of Fe I, Fe II, and Ca I lines, and using the wings of the strong, collisionally broaded Ca I 6162 Å line. Calculations were performed under the conditions of local thermodynamic equilibrium and plane-parallel geometry using the suite of Algol68 routines known as STARLINE68 (Craven 1974). Since this procedure followed closely that described by Smith & Drake (1987) and Drake & Smith (1991), we present here only a brief précis.

In their recent analysis of Pollux, Drake & Smith (1991) emphasized the importance of choosing model atmospheres with temperature structures appropriate to the stars in question. Since ϵ Eri is fairly close in spectral type to the Sun, we chose as basic model atmospheres a set of scaled solar models, derived by scaling the $T(\tau)$ relation of the Holweger & Müller (1974) solar model by the factor $T^{*}_{\rm eff}/T^{\odot}_{\rm eff}$. By virtue of their fixed temperature structures, scaled solar models cannot be used to account for the effects of different surface gravities and metallicities on derived abundances and line profiles. In order to treat the differential effects of surface gravity and metallicity, we employed a three-dimensional grid of model atmospheres, each dimension corresponding to one of the parameters $T_{\rm eff}$, log *g*, and global metallicity (represented by the abundance of iron relative to the Sun, [Fe/H]). These models were generated using the MARCS program, and are similar to those described

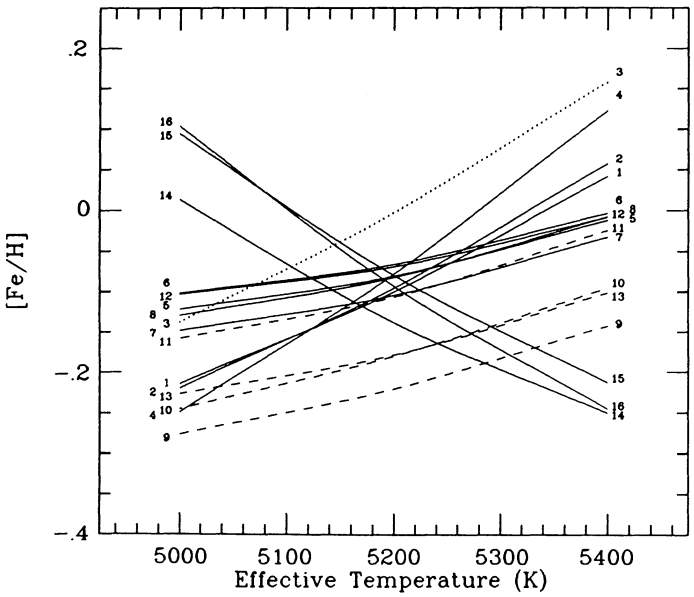

FIG. 2.—$T_{\rm eff}$-[Fe/H] diagram for ϵ Eri corresponding values of surface gravity and microturbulence log $g = 4.7$ and $\epsilon = 1.25$ km s^{-1}, respectively. Key to lines: (1) 5253.03, (2) 6151.62, (3) 6173.34, (4) 6498.95, (5) 5852.23, (6) 5855.09, (7) 5856.10, (8) 5858.79, (9) 5859.60, (10) 5862.37, (11) 6157.73, (12) 6159.38, (13) 6165.36, (14) 5264.81, (15) 6149.25, (16) 6456.39 Å. The four strongest lines in the sample of high-excitation Fe I lines are represented by the dashed curves (refer to text). The magnetically sensitive 6173 Å line is also shown (*dots*).

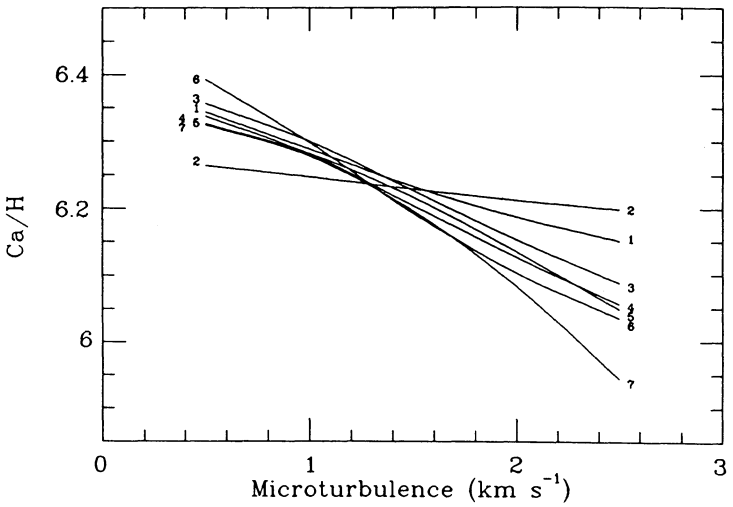

FIG. 3.—Logarithmic abundance against microturbulence diagram for ϵ Eri corresponding to the physical parameters $T_{\rm eff} = 5180$ K, log $g = 4.75$, and [Fe/H] = −0.1. Key to lines: (1) 5260.39, (2) 5867.57, (3) 6161.29, (4) 6166.44, (5) 6169.04, (6) 6455.60, (7) 6493.78 Å.

by Gustafsson et al. (1975) and published by Bell et al. (1976). The ranges of the stellar parameters were chosen so as to encompass the likely values of these quantities possessed by ϵ Eri and included the whole range of values listed in Table 1.

Using the two sets of model atmospheres, the effective temperature and iron abundance were determined simultaneously using the iron ionization balance, employing the usual method whereby the Fe I and Fe II lines are forced to yield the same abundance (see Fig. 2). In a similar way, the microturbulence and calcium abundance were determined by forcing Ca I lines of varying strength to yield the same abundance in the Ca-ξ plane (see Fig. 3). Smith & Drake (1987) and Drake & Smith (1991) have demonstrated that, provided the calcium abundance is known, the pressure-sensitive, collision-broadened wings of the Ca I 6162 Å line can provide a sensitive diagnostic of surface gravity in both late-type dwarfs and giants. The surface gravity was determined by varying this quantity until the theoretical 6162 Å profile matched the observed spectrum in the regions of the 6162 Å line wings (see Fig. 4). In practice, these three spectral indices used to determine $T_{\rm eff}$, log g, and microturbulence, ξ, are nonorthogonal, and the entire process proceeds by iteration until a self-consistent set of parameters is obtained.

Convergence of this procedure is usually obtained within three to four iterations. However, in the case of ϵ Eri, con-

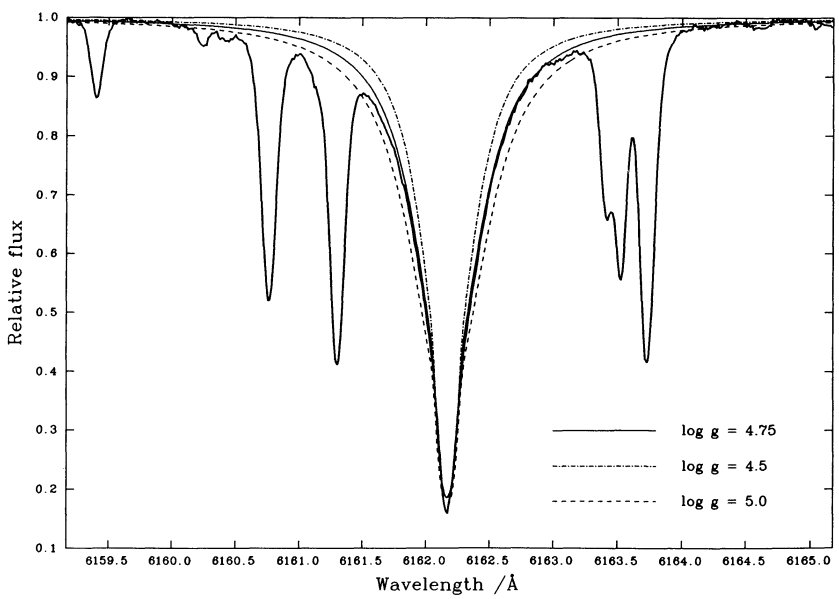

FIG. 4.—Ca 6162 profles: observed vs. various gravities, all profiles have $T_{\rm eff} = 5180$; [M/H] = [Ca/H] = −0.1

vergence was hamperered by an unusully large scatter in abundances derived from the Fe I lines. In the analysis of two solar-type dwarfs, τ Ceti and η Cas A, by Smith & Drake (1987), loci defined by the abundances derived from the set of Fe I and Fe II lines in the $T_{\rm eff}$-[Fe/H] plane were found to intersect sharply in a narrow "neck." The spread in the derived Fe abundances in the region of the "neck" was $\sim$0.05 dex. The corresponding $T_{\rm eff}$-[Fe/H] diagram for ϵ Eri, calculated for values of surface gravity and metallicity close to those finally adopted, is illustrated in Figure 2. The locus represented by the dotted curve corresponds to the Fe I 6173 Å line. This line is magnetically sensitive, and it comes as no surprise to us that it yields a spuriously high abundance, almost certainly due to the presence of strong magnetic fields. Indeed, Marcy (1984) used this line in an attempt to measure the surface magnetic field of ϵ Eri based on its additional Zeeman broadening. The 6173 Å line was, therefore, disregarded in the remainder of the analysis. The four strongest lines of the sample of high excitation Fe I lines, namely 5859, 5862, 6151, and 6165 Å, correspond to the dashed profiles. Disregarding the 6173 Å line, it is evident that there still exists a large spread in Fe I abundances, but that this spread would be reduced dramatically if the three lines at 5859, 5862, and 6165 Å were also disregarded. The remaining loci then converge sharply, intersecting in a narrow neck with a very small spread of $\sim$0.05 dex. Possible reasons for the apparent anomalies exhibited by the three high-excitation lines will be addressed in the next section. For the present, we proceed cautiously with the analysis, with the assumption that these lines are genuinely discrepant and can be disregarded.

Having adopted this standpoint, the derivation of the calcium abundance, microturbulence, and surface gravity proceeded straightforwardly. The final set of stellar parameters derived in this way was as follows:

$$T_{\rm eff} = 5180 \pm 50 \text{ K}$$
$$\log g = 4.75 \pm 0.1$$
$$[\text{Fe/H}] = -0.09 \pm 0.05$$
$$[\text{Ca/H}] = -0.10 \pm 0.05$$
$$\xi = 1.25 \pm 0.1 \text{ km s}^{-1}.$$

The errors quoted above are determined by the width of the "neck" in Figures 2 and 3 and by the resolution of the fit in Figure 4.

5. DISCUSSION

5.1. *Discrepant Lines of* Fe I

It was noted above that three of the high-excitation ($\chi \geq 3$ eV) lines of Fe I, at 5859, 5862, and 6165 Å, yielded abundances significantly lower than the rest of the Fe I lines. Possible reasons for these discrepancies are discussed below.

5.1.1. *Errors in Equivalent Widths*

In order to produce the observed abundance anomalies, of $\sim$0.1 dex, by erroneous measurement of equivalent widths, these would need to have been underestimated by 10% or so. Such an underestimate due to random error is extremely unlikely, this being much larger than the estimated uncertainty of $\leq$5% for these lines. Scattered light can be discounted as the source of an error of this magnitude since adjacent lines, and lines in the same Reticon exposures, do not exhibit anamolous behavior. Errors in continuum location can probably be discounted for similar reasons. While the spectrum of a K2 dwarf exhibits significantly more line crowding than does that of the Sun, potentially hampering continuum location, we have found that working at less crowded wavelengths longward of 5000 Å largely avoids continuum placement problems (e.g., see Fig. 1). Since our high signal-to-noise ratio spectra are fully resolved, any compromise due to line absorption features of regions used for continuum placement is readily apparent. In more quantitative terms, in order to have underestimated the equivalent widths of the discrepant lines by 10%, the error in continuum placement would need to have been of order 3% or so. Such an error is more than twice our estimated uncertainty in continuum placement for these lines.

5.1.2. *Photometric and Spectroscopic Variability*

As rotation changes the distribution of starspots on the visible hemisphere of a heavily spotted star, a modulation in surface brightness and line strengths might result—see Gray (1988) for a discussion. Soderblom & Däppen (1989) looked for a systematic variability with time in the photometry of ϵ Eri by Johnson et al. (1966) and found none. More recently, evidence for photometric variability was presented by Frey et al. (1991), who found a variability in BV photometry with a maximum amplitude of $\Delta V \sim 0.03$ mag, and with a period of 10–12 days. They attributed this variability to the presence of star spots. Toner & Gray (1988) claim to have discovered a large surface feature, dubbed a "starpatch," on the chromospherically active G8 dwarf ξ Boo A from a modulation of line asymmetries and equivalent widths. The amplitude in equivalent width variations of Fe I lines was reported to be 7% $\pm$ 1.5%. Interestingly, this amplitude is consistent with the magnitude of the abundance anomaly discovered here.

Our spectra of ϵ Eri were obtained on three separate nights, spanning a period of 4 days, with an additional observation made some 2 months later. The rotation period of ϵ Eri is known, with reasonable precision, to be 11.3 days (Baliunas et al. 1983, and references therein). We might, then, expect observable effects of rotational modulation in our spectra, obtained over approximately one-third of a rotation period, if such modulation exists. Such effects were sought by examining carefully the abundances derived from lines appearing in spectral regions observed on different nights, but no trends were found. We do not rule out such a rotational modulation, since our data lack sufficient temporal coverage. However, based on the evidence of our spectra, we would expect the amplitude of any rotational modulation in equivalent widths to be less than 10%.

5.1.3. *Incorrect Model Atmosphere Temperature Structure*

Since ϵ Eri is both chromospherically active and several hundred degrees cooler than the Sun, the immediate first choice of a scaled solar model, perhaps, requires further consideration. Interestingly, Holweger (1988) noted that abundances derived from Fe I lines in the spectrum of the chromospherically active dwarf ξ Boo A exhibited a large spread when compared to those derived from lines observed in the more quiescent dwarf 61 Vir, using the same instrumentation. Holweger remarks that some of the scatter could be removed by adopting a higher surface gravity, and by increasing the temperature of the appropriate scaled solar model by 200 K at optical depths $\log \tau < 0.1$, which he claims would not alter the effective temperature of the model. This modification would also raise the derived iron abundance, [Fe/H], from

-0.2 dex to solar, in keeping with the estimated youth of ξ Boo A.

The shapes of the wings of extremely strong spectral lines are sensitive to the distribution of temperature T with optical depth τ in a stellar atmosphere. This property has been exploited by previous workers in order to derive empirical T-τ relations for stars differing in spectral type from the Sun; see, for example, the analyses of Pollux, and of Procyon, by Ruland et al. (1980), and Steffen (1985), respectively, and references therein. Drake & Smith (1991) used the profile of the strongest, and least blended, of the Ca II infrared triplet transitions centered at 8542 Å to derive an empirical model atmosphere for the K0 giant Pollux. More recently, Smith, Lambert, & Ruck (1992) used the same line in order to assess the proprieties of different model atmospheres in their analysis of the subdwarf Groombridge 1830. The 8542 Å line was preferred because calcium is predominantly singly ionized at temperatures typical of late-type stellar photospheres, and there are good grounds for believing that the profiles of the triplet, apart from a narrow region of each line core, are formed in conditions very close to LTE (Jørgensen, Carlson, & Johnson 1992; Drake 1991). Following Drake & Smith, we have tested both the applicability of our scaled solar model, and of Holweger's suggested 200 K temperature enhancement, for our analysis of ϵ Eri, through a comparison of observed and theoretical 8542 Å line profiles. For additional interest, we calculated theoretical profiles for a MARCS model, and for the empirical model derived by Thatcher et al. (1991). The temperature structures of these models are illustrated in Figure 5. The Thatcher et al. model is, perhaps, primarily intended as a chromospheric model. The photospheric component is purported to be derived mainly by a trial-and-error attempt to model the shape of the Na D lines, using the Carlsson (1986) code MULTI and the atomic model of Kelch (1975).

The theoretical Ca II 8542 Å profiles calculated using the various models are illustrated in Figures 6*a* and 6*b*, together with the observed line profile. The MARCS, scaled solar, and modified scaled solar models were calculated for values of effective temperature and surface gravity close to those finally adopted. Atomic data were taken from Smith & Drake (1988). As expected from the work of Smith & Drake (1987), the theoretical profiles are insensitive to changes in $T_{\rm eff}$ by as much as 200 K and in log g by as much as 0.2 dex. Such changes are larger than our margin of error, so the fit to the observed profile cannot be improved by adjusting these parameters. The calculated profiles are much more sensitive to the metallicity parameter, and Figure 6*a* illustrates the effect of changing this parameter from metallicity [M/H] $= -0.1$, our optimum value, to metallicity [M/H] $= -0.4$, with corresponding change of the calcium abundance from Ca/H = 6.26 (based on the solar calcium abundance determined by Smith 1981) to Ca/H = 5.96. The scaled solar profile with slightly subsolar metallicity is the best fit to the wings of the observed profile. Our calculations indicate that an equally good fit to the observed profile could be obtained using a scaled solar profile corresponding to solar gravity (log $g = 4.44$) and solar metallicity. However, our investigation of the Ca I 6162 Å profile provided strong evidence in favor of a surface gravity about 0.3 dex higher than solar. For this reason we favor a metallicity about 0.1 dex below solar. The comparison between observed and calculated profiles in Figure 6*a* indicates that the metallicity is determined with an uncertainty of about 0.1 dex. The profile calculated with the MARCS model for [M/H] $= -0.1$ is slightly deeper in the line wings than the corresponding scaled solar profile: this is a consequence of the lower temperature at optical depths log $\tau < 0$ in the MARCS model (see Fig. 5), resulting in a lower Planck function.

All three calculated profiles shown in Figure 6*a* were computed for the LTE case and show deviations from the observed profile in the line core (< 1 Å from the line center). The infilling of the line core in the observed profile is most striking and is a well-known feature of chromospherically active stars (Linsky et al. 1979; Foing et al. 1989). Smith & Drake (1987) studied the 8542 Å line profile in the spectrum of the quiescent dwarf τ Ceti (spectral type G8), using the same instrumentation as adopted in the current investigation, and found the relative flux at the line center to be only about 0.3, i.e, the level of the abscissa in Figures 6*a* and 6*b*.

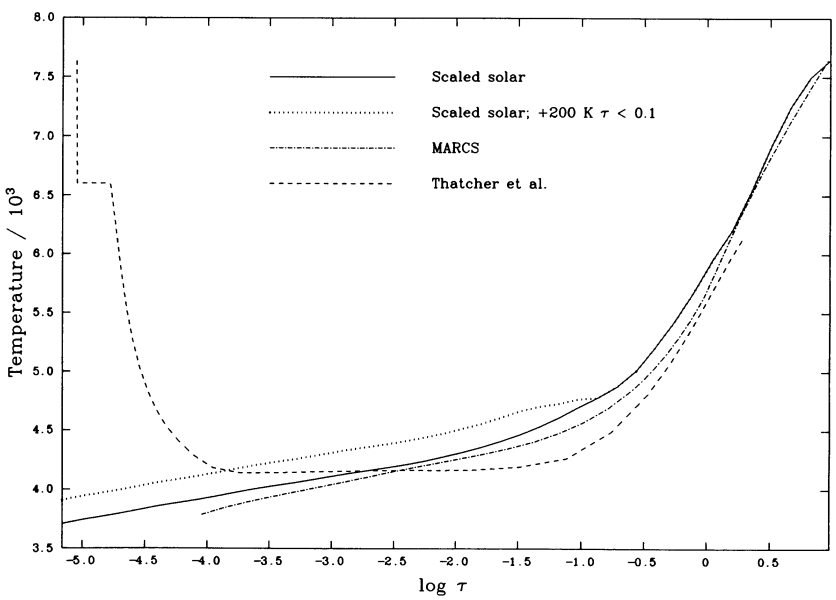

FIG. 5.—Temperature vs. log τ_{5000} for various model atmospheres

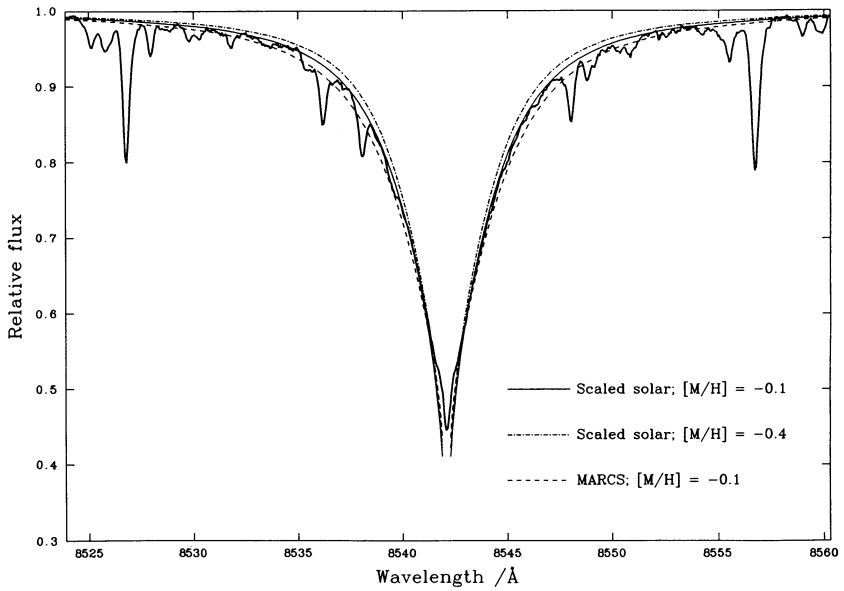

FIG. 6*a*

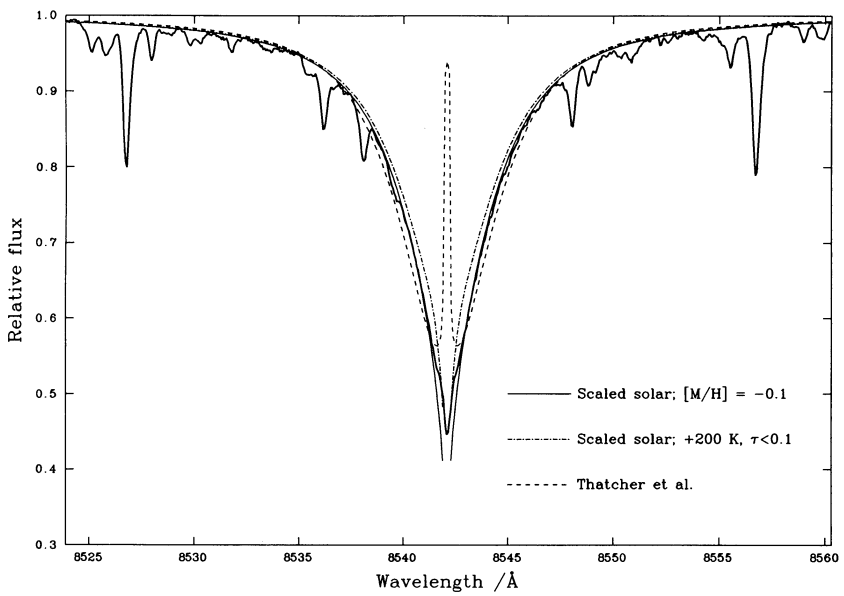

FIG. 6*b*

FIG. 6.—(*a*) Ca 8542 profiles: observed vs. scaled solar and MARCS; all profiles have $T_{\rm eff} = 5180$; $\log g = 4.75$; [M/H] = [Ca/H] as shown. (*b*) Ca 8542 profiles: observed vs. scaled solar, scaled solar with higher temperature at $\tau_{5000} < 0.1$, and Thatcher et al.; all profiles have $T_{\rm eff} = 5180$; $\log g = 4.75$; [M/H] = [Ca/H].

Figure 6*b* shows the observed profile and best-fit calculated profile compared to profiles computed using (1) a scaled solar model with temperature enhanced by 200 K at optical depths $\tau < 0.1$ and (2) the Thatcher et al. (1991) model. The profile corresponding to the modified scaled solar model is too shallow in the inner wing region and provides no evidence to support a temperature increase in the upper photosphere. Furthermore, we have recalculated our Fe abundances using this modified scaled solar model and found no significant improvement in the scatter of the results. The profile calculated using the Thatcher et al. model is slightly deep in the inner wings compared to the observed profile, and our LTE calculation produces a bright emission reversal in the line core. The chromospheric temperature rise of the model atmosphere has no effect on the calculated line wings and could be omitted from the model with little consequence. As explained above, the Thatcher et al. model was not primarily intended as a photospheric model and should not be judged as such. The non-LTE profile calculated by Thatcher et al. (see Fig. 3 of their paper) departs from the LTE profile in the line core region and predicts a narrow absorption core flanked by rather weak emission features. Thatcher et al. found no evidence for the narrow absorption core in their own observed profile which was recorded at lower resolution than the profile displayed here. An inspection of the core region in Figure 6*a* or 6*b* clearly shows the narrow absorption core with the emission features appearing as shoulders on each side.

Our study of the 8542 Å line profile has indicated, in agree-

ment with the findings of Steenbock (1983), that a scaled solar model derived from the Holweger & Müller solar atmosphere provides an appropriate temperature distribution for our analysis. We emphasize that the parts of the atmosphere of interest are mainly the deeper photospheric regions, where the weaker Ca I, Fe I, and Fe II lines central to our study are formed. These are the regions where the wings of the 8542 Å line profile (>2 Å from the line center) are formed and where the LTE approximation is valid. The comparison between the observed and calculated line wings favors metallicity [M/H] = −0.1, the same value as was indicated by the analyses of individual calcium and iron lines.

5.1.4. *Departures from LTE*

Of the four strongest lines in our sample of high-excitation Fe I lines, three are discrepant. This tends to suggest that non-LTE effects could be to blame: the cores of the stronger lines will be formed in higher photospheric layers than those of weaker lines and could be sampling parts of the atmosphere above the line thermalization depth. However, we have ruled out departures from LTE as being responsible for the observed anomalies for three reasons. First, the discrepant lines are still fairly weak at 82, 103, and 48 mÅ, and, were non-LTE effects to blame, we would also expect to see evidence of departures from LTE in the low-excitation lines of comparable strength formed in similar and higher photospheric layers (as, for example, found empirically in the spectrum of the K0 giant Pollux by Ruland et al. 1980 and Drake & Smith 1991). Second, since we have used "solar" oscillator strengths for the Fe lines in our sample, any non-LTE effects in our abundance results would be residual effects *relative to the Sun*. Such a relative non-LTE effect of the magnitude observed would seem most unlikely. Third, we have investigated the effects of departures from LTE quantitatively: for the Holweger & Müller (1974) solar atmosphere and a scaled solar model corresponding to the parameters derived in our analysis, listed above, the radiative transfer and statistical equilibrium equations were solved for a model iron atom using a modified edition of the code MULTI (Carlsson 1986). The model atom, an updated version of that used by Steenbock (1985), comprised 74 levels of Fe I, 24 levels of Fe II, and the Fe III continuum, with 75 bound-bound radiative transitions treated in detail. The effects of line blanketing on the ionizing radiation field were included using the opacity distribution functions of Kurucz (1979), and collisional interactions with neutral hydrogen atoms were taken into account using the prescription of Steenbock & Holweger (1984). For all of the Fe I lines in our sample, the difference in non-LTE abundance corrections, $Fe/H_{NLTE} - Fe/H_{LTE}$, derived for the solar model and the model appropriate to ϵ Eri were less than 0.05 dex. Tests were also made of the effects of a chromospheric temperature rise by including the Thatcher et al. chromosphere on top of our scaled solar model. In the case of all the lines, the derived non-LTE abundances were changed by less than 0.01 dex.

5.1.5. *Photospheric Inhomogeneities*

Studies of stellar spectral line bisectors suggest that the granulation thermal contrast in dwarf stars increases with increasing temperature (see, for example, Gray 1988). These conclusions have been confirmed theoretically by sophisticated hydrodynamical models which are now able to reproduce in some detail the characteristics of observed spectral line shapes and asymmetries—see, for example, the recent series of papers by Dravins & Nordlund (1990 and references therein). This, in turn, suggests that spectral lines in the solar photosphere are probably formed over a wider range of thermal conditions than are their counterparts in a K2 dwarf. Since a plane-parallel, homogeneous model, such as those used in this analysis, is simply an average of the complex thermal structure of a stellar photosphere, such effects are not accounted for explicitly in traditional model atmosphere analyses. It is possible, then, that systematic errors might be introduced into our analysis through inadequacies of the one-dimensional modeling of a K2 dwarf relative to the Sun. Because granulation velocities are observed to decrease with increasing height, the effects of photospheric thermal inhomogeneities on spectral lines of a given species depend primarily on line strength and excitation (e.g., Pierce & Breckinridge 1973; Glebocki & Stawikowski 1980; Dravins, Lindegren, & Nordlund 1981; and Nadeau 1988). Therefore, one might expect that spectral lines which sample different ranges of photospheric depths, such as weak and strong Fe I lines, will be affected by our neglect of photospheric inhomogeneities to different extents.

Two facts argue against such an explanation for the Fe I line anomalies uncovered in this study. First, two of our lines, namely 6157.73 Å and 5858.23 Å, are both of high excitation and have comparable line strengths to the discrepant lines, yet yield abundances which are in concordance with the weaker Fe I lines. Second, in similar analyses of the K2 dwarf α Cen B (Smith et al. 1986), and of the G8 dwarf τ Ceti (Smith & Drake 1987), no such discrepancies in the Fe I lines were found.

There is some evidence which suggests that granulation is suppressed somewhat with increasing magnetic field strength (e.g., Livingston 1982; Kaisig & Schröter 1983; Cavallini, Ceppatelli, & Righini 1988), in which case one might expect still further systematic differences between the solar case and that of a magnetically active, cooler dwarf. However, our two concordant Fe I lines listed above again argue contrary to such an explanation.

5.1.6. *Chromospheric Activity*

The possible reasons for the discrepancies in the high excitation Fe I lines considered thus far all appear rather unlikely. As we mentioned above, in analyses of the quiescent, but otherwise very similar dwarfs, α Cen B and τ Ceti, Smith et al. (1986) and Smith & Drake (1987), respectively, found no such anomalous behavior. Since the only major difference between these stars and ϵ Eri lies in their levels of chromospheric activity, the most obvious cause of a discrepancy would seem to be directly related to this phenomenon.

A large body of evidence shows that magnetic fields engender chromospheric and coronal emission; see Gray (1988) for a recent review. Since the magnetically sensitive 6173 Å line of Fe I was found to yield an overabundance, it is possible that there are further magnetic influences in our abundance results. We investigated this possibility by searching for a correlation of derived abundance with Landé g factor. None was evident. Using what appears to be the same spectroscopic material as analyzed by Steenbock (1983), Steenbock & Holweger (1981) also investigated whether or not such a correlation was present in their spectra of ϵ Eri and found none.

Kelch, Linsky, & Worden (1979) suggest that the chromospheres of ϵ Eri and ξ Boo A are similar in structure near the temperature inversion to a typical solar plage region. Both strong and weak lines are filled in by the emission excess in plage regions (e.g., see LaBonte & Rose 1985 for a discussion), but the degree of infilling is relatively insensitive to line excita-

tion. Therefore, we do not expect the presence of plages to be the *direct* cause of the anomalous behavior observed here.

Cayrel, Cayrel de Strobel, & Campbell (1985) derived below solar metallicites for chromospherically active dwarfs in the Hyades cluster. They considered their results anamolous in view of the supposed youth of the Hyades and suggested that the chromospheric temperature rise at the base of the photosphere could be responsible by causing an infilling, and therefore weakening, of spectral lines. Our non-LTE calculations for a scaled solar model with and without the chromosphere of Thatcher et al. (1991), described above, produced essentially identical abundances. We conclude from this that the effect of the chromospheric temperature rise *alone* cannot produce anomalies of the magnitude observed. It is possible, however, that Cayrel et al. observed a similar effect to that observed here, and that the large variation in derived Fe I abundances, evident from our very high quality spectra, was masked by the larger random scatter in derived abundances inevitably present from their lower resolution spectra. If some lines were then yielding underabundances, as suggested here, an average of their derived abundances would indeed result in a spurious abundance underestimate.

Another possible chromospheric effect to be considered is line fluorescence. The criteria for line fluorescence are explained clearly by Gahm (1974). Stated simply, fluorescence of a line with lower and upper levels i and j can occur if absorption of an "emission" flux (i.e., a flux greater than that due to the local Planck function at the wavelength in question, and esentially monochromatic in character) by a transition of lower level k and upper level j (i.e., the same upper level) is possible; the upper level j becomes overpopulated relative to its Boltzmann population, and may decay by the route $j \rightarrow i$, resulting in line filling and a reduced equivalent width. Candidate lines for causing fluorescence in Fe I were sought in the lists of astrophysically common emission lines of Meinel, Areni, & Stockton (1969) and Gahm (1974). We came across no favorites since there appear to be no obvious pumping routes in Fe I which would explain the infilling of the three discrepant lines observed here.

At present, a mechanism of this type is the only explanation considered here which we cannot with any certainty rule out. It seems unlikely that high excitation Fe I lines, which are formed relatively deep in the photosphere, would be affected by the presence of a chromosphere. However, a nonthermal mechanism is the only effect which could produce the pattern of Fe abundances which we observe. We therefore suggest tentatively that the source of the discrepancy lies in a nonthermal excitation of Fe I which is related to chromospheric activity. A theoretical investigation into such nonthermal excitation is currently in progress.

5.2. *Stellar Parameters*

5.2.1. *Effective Temperature*

Our effective temperature lies at the high end of the values derived and adopted by previous workers. Except for those derived by Krishna Swamy (1966) and Burnashev (1983), the earlier values were all based on narrow- or broad-band multicolor photometry. Burnashev states that his method, based on scanner observations of a stellar spectral energy distribution, is comparable in accuracy to methods employing narrow-band indices. Photometric temperature determinations for late-type stars are typically accompanied by claimed uncertainties of about ± 100 K. Arribas & Martinez Roger (1989) claim an accuracy of ± 160 K on their recent calibration. Considering such uncertainties brings the majority of the values cited in Table 1 into agreement with our own value.

We should point out that, as has been discussed in the literature on previous occasions (e.g., Gustafsson & Gråe-Jørgensen 1985), our spectroscopic effective temperature is based on a model atmosphere label temperature and is not strictly related to the stellar integrated flux. Our iron ionization balance method using solar gf-values ensures that, for spectral types very similar to the Sun, the label temperature will be identical to the true effective temperature. For spectral types differing significantly from solar, it is possible that systematic differences between the label and true effective temperatures might arise. Of course, even if this should be the case, the spectroscopic label temperature would be the appropriate quantity to use in model atmosphere analyses. Since, through careful analysis of the Ca II 8542 Å line, we have verified that the temperature structure of a scaled solar model atmosphere is appropriate for ϵ Eri, we feel that, in the present case, any significant systematic difference between our spectroscopic label and the true effective temperatures are unlikely. Moreover, the trend in previous studies of this nature (e.g., Smith & Drake 1987; Drake & Smith 1991) is for our spectroscopically derived effective temperatures to agree with the most recent and reliable photometric determinations—see Smith (1992) for a discussion. We find a similar situation in the present case for ϵ Eri. Of the photometric endeavors, by virtue of the method, the temperature of Bell & Gustafsson (1989) based on the IRFM is probably superior to the others. When applied correctly, the IRFM can probably achieve an accuracy of 1% or better (Blackwell et al. 1986). It is encouraging then that the temperature of Bell & Gustafsson is in excellent agreement with our spectroscopic value.

5.2.2. *Surface Gravity*

In the case of field stars which are not members of binary or multicomponent systems, the parameter which is often most uncertain is the surface gravity. This is true for the existing estimates of this parameter in the case of ϵ Eri, which exhibit a scatter over a factor of 5. None of these estimates can realistically claim an uncertainty of better than $\sim \pm 0.3$ dex. Kelch (1978) declared that there was only one existing estimate of the surface gravity of ϵ Eri prior to his own—that of Krishna Swamy (1966)—and apparently overlooked the endeavours of Hearnshaw (1974) and Oinas (1974a, b). The uncertainty of ± 0.1 dex he quotes for his value must be considered a trifle optimistic. There appear to have been only two spectroscopically derived surface gravities, those of Oinas and of Steenbock (1983). Although both used the Fe I–Fe II ionization equilibrium, Steenbock's is by far the best determined. Oinas derived unrealistically low surface gravities for all of his sample of K dwarfs, including $\log g = 3.6$ for ϵ Eri, and adopted instead arbitrary values for his abundance calculations. Steenbock's value is not in agreement with our own. He remarks, however, that due to the temperature sensitivity of the Fe ionization equilibrium, a 50 K increase in the effective temperature would lead to a surface gravity higher by ~ 0.1 dex. Substituting the adopted temperature of Steenbock with that derived in this study would raise his value of surface gravity to $\log g \approx 4.5$. In tandem with the uncertainty of ± 0.3 dex Steenbock ascribed to his surface gravity determinations, this result would then be in marginal agreement with our own.

5.2.3. *Microturbulence*

Microturbulence is often overlooked as a stellar parameter, most probably because—provided weak lines are used—its influence in abundance analyses is not catastrophically large. We see from Table 1 that only four attempts have been made to determine the microturbulence parameter for ϵ Eri. The value adopted by Oinas is poorly explained, and it is difficult to make an estimate of its credibility. Hearnshaw based his microturbulence estimates on comparisons between solar and stellar spectra. In the case of ϵ Eri he adopted a value of 1.3 km s^{-1}, the same value he adopted for the Sun. As mentioned above, Steenbock (1983) appears to have based his analysis on the same spectroscopic material as did Steenbock & Holweger (1981), and results from both of these studies are very similar.

Steenbock & Holweger (1981) derived a microturbulent velocity $\xi = 1.9 \pm 0.2$ km s^{-1} from their set of Fe I lines by adjusting ξ until weak and strong lines yielded the same iron abundance. They suggested that photospheric microturbulence could be a spectroscopic manifestation of acoustic waves which heat the chromosphere, pointing out that their derived microturbulence values for the chromospherically more quiet stars τ Ceti and 40 Eri A were significantly lower at 1.5 and 1.3 km s^{-1}, respectively. Steenbock (1983) remarked on the gravity dependence of his results: raising log g by 0.3 dex lowered ξ by 0.2 km s^{-1}. However, even with Steenbock's surface gravity revised upward, as above, the microturbulent velocity would still be slightly higher than that derived here.

In order to verify the microturbulent velocity derived here using our set of Ca I lines, we have plotted our derived iron abundances, [Fe/H], as a function of ξ for the set of Fe I lines. This plot is illustrated in Figure 7. The high-excitation lines suspected of being discrepant correspond to the dashed curves, and the dotted curve corresponds to the magnetically sensitive 6173 Å line. Neglecting these curves, the microturbulence indicated by the confluence of the remaining loci is $\xi = 1.2 \pm 0.1$ km s^{-1}, in excellent agreement with the result derived from the set of Ca I lines. This value of microturbulence is the same as the value $\xi = 1.25$ km s^{-1}, derived for the quiescent dwarf τ Ceti by Smith & Drake (1987). Contrary to the suspicions of Steenbock & Holweger (1981), this result suggests no correlation between microturbulence and chromospheric activity.

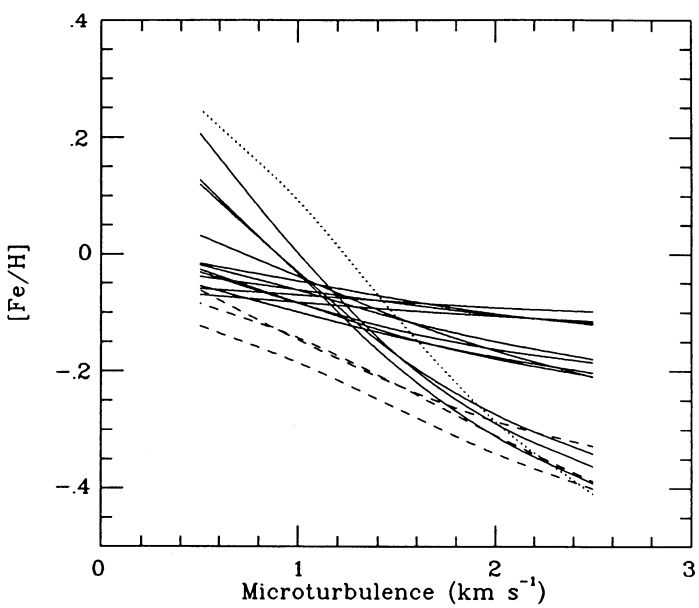

FIG. 7.—Logarithmic abundance against microturbulence diagram for the sample of Fe lines in ϵ Eri corresponding to the adopted values for the physical parameters: $T_{\rm eff} = 5180$ K and log $g = 4.75$. The high-excitation lines of Fe I found to be discrepant are illustrated (*dashed curves*), as well as the magnetically sensitive 6173 Å (*dots*).

5.2.4. *Metallicity*

Spectroscopic methods, when applied correctly, are almost certainly capable of higher accuracy in deriving element abundances than are those based on photometric indices—see the exhortation of Griffin & Holweger (1989). The earlier work of Oinas (1974a, b) and Hearnshaw (1974) is probably superseded in accuracy by the more recent study of Steenbock (1983), who benefited from a more advanced model atmosphere analysis. All of these endeavors used photographic spectra. Hearnshaw used blue spectral regions, choosing windows for continuum location from the Utrecht atlas of the solar spectrum (Minnaert, Mulders, & Houtgast 1940). Working in the blue, however, is still perilous: Holweger (1970) has pointed out that continuum windows in the solar spectrum probably do not exist shortward of 4000 Å; the situation can only be compounded in later spectral types. Oinas, in a somewhat confusing analysis, obtained wildly different iron abundances from lines due to Fe I and Fe II—a problem inextricably linked with his very low surface gravity estimate (see above). Steenbock used yellow spectral regions, and, again, his abundances are the best determined. Comparing his value for the iron abundance, [Fe/H] = -0.23 ± 0.07, with our own, reveals only a slight disagreement. This disagreement could be entirely removed by replacing Steenbock's effective temperature with that derived in this study.

5.2.5. *Age and Mass*

We mentioned in § 1 the papers by Guenther (1987) and Soderblom & Däppen (1989), whose basis is the purported measurements of p-mode oscillations by Noyes et al. (1984), which raise a dichtomy over the age of ϵ Eri. We point out that the Noyes et al. observations still lack independent confirmation. Nevertheless, these papers raised some interesting points, and we refer to them here for completeness.

Guenther (1987) presented three different models which fitted the Noyes et al. oscillation spectrum: the first of these had an age of 10 Gyr, $Z = 0.013$ ([Fe/H] = -0.19), and a mixing length $\alpha = 1.00$—lower than the canonical solar value; the second suggested a young star, but provided that ϵ Eri was less luminous than has been measured due to binarity—a possibility no longer likely since the very accurate radial velocity survey of Campbell et al. (1988); the third suggested that the metal abundance of ϵ Eri has been underestimated due to line filling caused by plages, and that it is a young star with $Z = 0.032$ ([Fe/H] = $+0.2$). The argument that ϵ Eri might be an old star is based on its apparently below solar metallicity, as derived by Hearnshaw (1974) and Oinas (1974a, b)—see Table 1. The only grounds for this argument appear to be the age-metallicity relation for the solar neighborhood derived by Twarog (1980). However, it has been pointed out before (e.g., Lambert 1989) that this relation exhibits considerable scatter, and that such a mild metal deficiency as exhibited by ϵ Eri should only be used as a statistical age diagnostic. Soderblom & Däppen (1989) adopted a different bolometric correction which produced a less luminous star by 0.09 mag. They considered the observed chromospheric activity as con-

straining the age to ~1 Gyr, and subsequently had no difficulty in reconciling their adopted luminosity and temperature with a zero-age main-sequence (ZAMS) model. However, in order then to fit the purported oscillation spectrum, a mixing length $\alpha \sim 0.5$ was required. Both Guenther (1987) and Soderblom & Däppen (1989) point to work by Tayler (1987), which suggests that relatively high rotation rates and strong magnetic fields might inhibit convection, resulting in an effectively lower mixing length.

Our new values for the parameters $T_{\rm eff}$, log g, and [Fe/H], combined with existing measurements of luminosity, can be compared with theoretical evolutionary models. From the effective temperature and luminosity, an estimate of the radius, R, may be derived:

$$\log \frac{L_*}{L_\odot} = 4 \log \frac{T_*}{T_\odot} + 2 \log \frac{R_*}{R_\odot} .$$

Soderblom & Däppen adopt $\log L_*/L_\odot = -0.48 \pm 0.04$, based on the photometry of Johnson (1966) and Johnson et al. (1966), although they note that choosing the bolometric correction of Hayes (1978) would yield $\log L_*/L_\odot = -0.43 \pm 0.04$. We adopt the former value, though we admit the possibility of a slightly larger uncertainty so as not to preclude the lower value. Using our effective temperature $T_{\rm eff} = 5180$ K, our value for the radius of ϵ Eri is then

$$\log \frac{R_*}{R_\odot} = -0.15 \pm 0.06 .$$

Combined with our value for the surface gravity, log $g = 4.75 \pm 0.1$, we obtain for the mass

$$\log \frac{M_*}{M_\odot} = 0.0 \pm 0.1 \; ; \quad \frac{M_*}{M_\odot} = 1.0 \pm 0.3 .$$

We have compared our set of parameters with the ZAMS isochrones of VandenBerg & Bridges (1984). The result is illustrated in Figure 8. Our effective temperature, surface gravity, and metallicity are entirely consistent with a ZAMS model of mass $M_*/M_\odot = 0.85$. Moreover, our spectroscopically derived mass is also in good agreement with this result. Coupled with the evidence of high chromospheric activity and brisk rotation, the above estimates suggest that ϵ Eri is almost certainly a young star of slightly less than one solar mass.

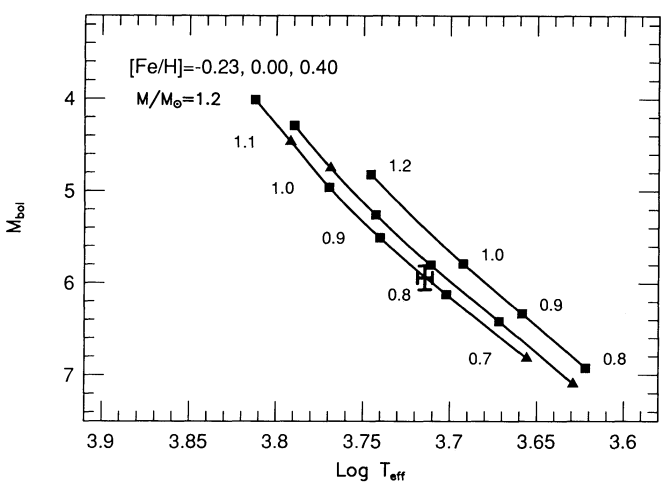

FIG. 8.—Zero-age main-sequence models from VandenBerg & Bridges (1984) for a range of stellar mass and metallicity. The error bar represents the uncertainties in the parameters of ϵ Eri: $M_{\rm bol}$ is from the literature (see text); $T_{\rm eff}$ is from this work.

6. CONCLUSIONS

By means of a detailed model atmosphere analysis of high-quality spectroscopic recordings of calcium and iron lines, we have derived a set of self-consistent atmospheric parameters for the chromospherically active dwarf ϵ Eri. The results obtained, and in particular the value for surface gravity derived from the collisionally broadened wings of the Ca I 6162 Å line, represent a significant improvement in accuracy over existing estimates of these parameters. The metallicity indicated by a careful analysis of neutral and ionized lines of iron is entirely consistent with that determined from a detailed comparison between theoretical and observed profiles of the metallicity-sensitive Ca II 8542 Å line. The shape of this line profile indicates that the temperature-depth relation of a scaled solar model atmosphere is appropriate for ϵ Eri.

Three high-excitation lines of Fe I, at 5859, 5862 and 6165 Å, are found to be discrepant in the sense that they yield abundances which are approximately 0.1 dex lower than those derived from the bulk of the Fe I lines. We postulate that this is a result of nonthermal excitation of Fe I caused by chromospheric emission. If such an effect is widespread among chromospherically active stars, then abundance analyses of these stars could be underestimating the iron abundance by 0.15 dex or so.

The magnetically sensitive Fe I 6173 Å line has yielded an iron abundance which is approximately 0.1 dex higher than that derived from magnetically insensitive Fe I lines. This effect is almost certainly a result of Zeeman broadening arising as a result of a relatively strong surface magnetic field, such as has been documented in many previous studies.

The physical parameters derived in this study are perfectly consistent with those predicted by a 0.8 $M_\odot$ ZAMS theoretical evolutionary model of VandenBerg & Bridges (1984). This evidence, coupled with a relatively high rotation rate, strong magnetic field, and high chromospheric activity, suggests emphatically that ϵ Eri is a young star of slightly less than 1 solar mass.

Finally, if the purported oscillation spectrum of Noyes et al. (1984) has been interpreted correctly by Guenther (1987) and Soderblom and Däppen (1989), then the parameters derived here imply that stellar models for ϵ Eri probably require a significantly subsolar mixing length.

We wish to thank the Director of the McDonald Observatory for granting facilities for our observations. It is a particular pleasure to record our gratitude for the warm hospitality and help received from the following members of the Astronomy Department at the University of Texas: Professor D. L. Lambert, V. V. Smith, and J. Tomkin, who also undertook additional observations on our behalf. Y. Chmielewski is thanked for kindly supplying routines to calculate model atmospheres from given $T(\tau)$ relations. M. Lemke is thanked for kindly supplying some atomic data for non-LTE calculations. We gratefully acknowledge the generosity of Professor B. Gustafsson in making the MARCS suite of programs available to the UK STARLINK network, and we extend our thanks to A. E. Lynas-Gray for implementing these programs at Oxford. G. S. wishes to thank the Royal Society of London, the Astor Fund, and Oxford University for providing support

for his visit to Texas. J. J. D. gratefully acknowledges support from an SERC studentship and subsequently a NATO Postdoctoral Fellowship while engaged in some of this work, and support for publication charges from NASA contract NAS5-30180, administered by the Center for EUV Astrophysics at UC Berkeley. Finally, we wish to thank the anonymous referee for pertinent comments which enabled us to improve the manuscript.

REFERENCES

Abia, C., Rebolo, R., Beckman, J. E., & Crivellari, L. 1988, A&A, 206, 100
Arribas, S., & Martinez Roger, C. 1989, A&A, 215, 305
Aumann, H. H. 1985, PASP, 97, 885
Baliunas, S. L., et al. 1983, ApJ, 275, 752
Barry, D. C., Cromwell, R. H., & Hege, E. K. 1987, ApJ, 315, 264
Bell, R. A., Eriksson, K., Gustafsson, B., & Nordlund, Å. 1976, A&AS, 23, 37
Bell, R. A., & Gustafsson, B. 1989, MNRAS, 236, 653
Blackwell, D. E., Booth, A. J., Petford, A. D., Leggett, S. K., Mountain, C. M., & Selby, M. J. 1986, MNRAS, 221, 427
Bohigas, J., Carrasco, L., Torres, C. A. O., & Quast, G. R. 1986, A&A, 157, 278
Burnashev, V. I. 1983, Izv. Krym. Astrofiz. Obs., 67, 13
Campbell, B., Walker, G. A. H., & Yang, S. 1988, ApJ, 331, 902
Carlsson, M. 1986, A Computer Program For Solving Multi-level non-LTE Radiative Transfer Problems In Moving Or Static Atmospheres, Uppsala Astron. Obs. Report, 33
Cavallini, F., Ceppatelli, G., & Righini, A. 1988, A&A, 205, 278
Cayrel, R., Cayrel de Strobel, G., & Campbell, B. 1985, A&A, 146, 249
Cayrel de Strobel, G., Bentolila, C., Hauck, B., & Duquennoy, A. 1985, A&AS, 59, 145
Craven, P. G. 1974, D.Phil thesis, Univ. of Oxford
Drake, J. J. 1991, MNRAS, 251, 369
Drake, J. J., & Smith, G.1991, MNRAS, 250, 89
Dravins, D., Lindgren, L., & Nordlund, Å. 1981, A&A, 96, 345
Dravins, D., & Nordlund, Å. 1990, A&A, 228, 218
Foing, B. H., Crivellari, L., Vladilo, G., Rebolo, R., & Beckman, J. E. 1989, A&AS, 80, 189
Frey, G. J., Grim, B., Hall, D. S., Mattingly, P., Robb, S., Wood, J., & Zeigler, K. 1991, AJ, 102, 1813
Frisk, U. 1983, Ph.D. thesis, Stockholm Univ.
Gahm, G. F. 1974, A&AS, 18, 259
Gillet, F. C. 1986, in Light on Dark Matter, ed. F. Israel (Dordrecht: Reidel), 61
Glebocki, R., & Stawikowski, A. 1980, in IAU Coll. 51, Stellar Turbulence, ed. D. F. Gray & J. L. Linsky (Heidelberg: Springer-Verlag), 55
Gray, D. F. 1988, Lectures On Spectral Line Analysis: F, G, and K Stars (Arva, Ontario: The Publisher)
Griffin, R. E. M., & Holweger, H. 1989, A&A, 214, 249
Guenther, D. B. 1987, ApJ, 312, 211
Guenther, D. B., & Demarque, P. 1986, ApJ, 301, 207
Gustafsson, B., Bell, R. A., Eriksson, K., & Nordlund, Å, 1975, A&A, 42, 407
Gustafsson, B., & Gråe-Jørgensen, U. 1985, in IAU Symp. 111, Fundamental Parameters and Models of Stellar Atmospheres, ed. D. S. Hayes, L. E. Pasinetti, & A. G. Davis Philip (Dordrecht: Reidel), 303
Hayes, D. S. 1978, in IAU Symp. 80, The HR Diagram, ed. A. G. Davis Philip & D. S. Hayes (Dordrecht: Reidel), 65
Hearnshaw, J. B. 1974, A&A, 34, 263
Holweger, H. 1970, A&A, 4, 11
———. 1988, in IAU Symp. 132, The Impact of Very High S/N Spectroscopy on Stellar Physics, ed. G. Cayrel de Strobel & M. Spite (Dordrecht: Kluwer), 411
Holweger, H., & Müller, E. A. 1974, Sol. Phys., 39, 19
Johnson, H. L. 1966, ARA&A, 4, 193
Johnson, H. L., Mitchell, R. I., Iriarte, B., & Wisńiewski, W. Z. 1966, Comm. Lunar Planet. Lab., 4 (63), 99
Jordan, C., Ayres, T. R., Brown, A., Linsky, J. L., & Simon, T. 1987, MNRAS, 225, 903
Jørgensen, U. G., Carlsson, M., & Johnson, H. R. 1992, A&A, 254, 258
Kaisig, M., & Schröter, E. H. 1983, A&A, 117, 305
Kelch, W. L. 1975, ApJ, 195, 679
———. 1978, ApJ, 222, 931
Kelch, W. L., Linsky, J. L., & Worden, S. P. 1979, ApJ, 229, 700
Krishna Swamy, K. S. 1966, ApJ, 145, 174
Kurucz, R. L. 1979, ApJS, 40, 1
Kurucz, R. L., Furenlid, I., Brault, J. W., & Testerman, L. 1984, Solar Flux Atlas from 596 to 1300 nm (National Solar Observatory Atlas No. 1) (Sunspot, NM: National Solar Observatory)
Kurucz, R. L., & Peytremann, E. 1975, Smithsonian Astrophys. Obs. Spec. Rep. 362
LaBonte, B. J., & Rose, J. A. 1985, PASP, 97, 790
Lambert, D. L. 1989, in Cosmic Abundances of Matter, ed. C. J. Waddington (AIP Conf. Proc. 183) (New York: AIP), 168
Leroy, J. L., & Le Borgne, J. F. 1989, A&A, 223, 336
Livingston, W. C. 1982, Nature, 297, 208
Linsky, J. L., Hunten, D. M., Sowell, R., Glackin, D. L., & Kelch, W. L. 1979, ApJS, 41, 481
Marcy, G. W. 1984, ApJ, 276, 286
Marcy, G. W., & Basri, G. 1989, ApJ, 345, 480
Mathys, G., & Solanki, S. K. 1989, A&A, 208, 189
Meinel, A. B., Aveni, A. F., & Stockton, M. W. 1969, Catalogue of Emission Lines in Astrophysical Objects (2d ed.; Tucson: Optical Sciences Center and Steward Observatory, Univ. Of Arizona)
Minnaert, M., Mulders, G. F. W., & Houtgast, J. 1940, Photometric Atlas of the Solar Spectrum 3332 Å to 8771 Å (Amsterdam: Schnabel)
Nadeau, D. 1988, ApJ, 325, 480
Noyes, R. W., Baliunas, S. L., Belserene, E., Duncan, D. K., Horne, J., & Widrow, L. 1984, ApJ, 285, L23
Oinas, V. 1974a, ApJS, 27, 391
———. 1974b, ApJS, 27, 405
Pierce, A. K., & Breckinridge, J. B. 1973, The Kitt Peak Table of Photographic Solar Wavelengths (Kitt Peak Obs. Contr., 559)
Ruland, F., Griffin, R., Griffin, R., Biehl, D., & Holweger, H. 1980, A&AS, 42, 391
Saar, S. H. 1988, ApJ, 324, 441
Simon, T., Kelch, W. L., & Linsky, J. L. 1980, ApJ, 237, 72
Skumanich, A. 1972, ApJ, 171, 565
Smith, G. 1981, A&A, 103, 351
———. 1988, J. Phys. B, 21, 2827
———. 1992, in Elements and the Cosmos, ed. R. J. Terlevich & M. G. Edmunds (Cambridge: Cambridge Univ. Press), 142
Smith, G., & Drake, J. J. 1987, A&A, 181, 103
———. 1988, MNRAS, 231, 115
Smith, G., Edvardsson, B., & Frisk, U. 1986, A&A, 165, 126
Smith, G., & Lambert, D. L. 1983, A&A, 117, 177
Smith, G., Lambert, D. L., & Ruck, M. J. 1992, A&A, in press
Smith, G., & Raggett, D.St.J. 1981, J. Phys. B, 14, 4015
Soderblom, D. R., & Däppen, W. 1989, ApJ, 342, 945
Steenbock, W. 1983, A&A, 126, 325
———. 1985, in Cool Stars With Excesses of Heavy Elements, ed. M. Jaschek & P. C. Keenan (Dordrecht: Reidel), 231
Steenbock, W., & Holweger, H. 1981, A&A, 99, 192
———. 1984, A&A, 130, 319
Steffen, M. 1985, A&AS, 59, 403
Tayler, R. J. 1987, MNRAS, 227, 553
Thatcher, J. D., Robinson, R. D., & Rees, D. E. 1991, MNRAS, 250, 14
Tomkin, J., & Lambert, D. L. 1980, ApJ, 235, 925
Toner, C. G., & Gray, D. F. 1988, ApJ, 334, 1008
Twarog, B. A. 1980, ApJ, 242, 242
VandenBerg, D. A. 1985, ApJS, 58, 711
VandenBerg, D. A., & Bridges, T. S. 1984, ApJ, 278, 679
Vogt, S. S., Tull, R. G., & Kelton, P. 1978, Appl. Opt., 17, 574
Walker, H. J., & Wolstencroft, R. D. 1988, PASP, 100, 1509